

Title No. 115-S63

Modeling Beam-Membrane Interface in Reinforced Concrete Frames

by Vahid Sadeghian, Oh-Sung Kwon, and Frank Vecchio

Multi-scale analysis, which involves combining advanced elements with computationally fast elements, is an effective method for assessing the behavior of large structures with deficient or complex members. One major challenge in multi-scale analysis is modeling the interface between the two types of elements. This study presents a new interface element for connecting a beam element to membrane elements, specifically formulated for reinforced concrete members. The proposed element considers reinforced concrete a composite material, is capable of computing linear and nonlinear stress distributions through the section, and allows for transverse expansion at the interface section. The accuracy of the interface element is verified through analysis of a series of beam specimens presented in the literature. The improvements of the proposed method are compared against two commonly used beam-membrane coupling methods. Lastly, the application of the interface element is demonstrated by multi-scale analysis of a reinforced concrete frame structure with critical joints.

Keywords: beam-membrane coupling; multi-scale modeling; nonlinear analysis; reinforced concrete; shear behavior.

INTRODUCTION

In nonlinear finite element analysis, situations often arise where more than one type of element is required to model the structural system. This type of simulation is known as multi-scale or mixed-type modeling and has attracted much research interest over the past several years.¹⁻⁸ One common application of mixed-type modeling is connecting beam elements and membrane elements for analysis of large, complex reinforced concrete structures. Beam elements are computationally fast and suitable for global analysis of structures. However, due to the limitations of their formulations, they are unable to accurately analyze members with highly nonlinear behavior (for example, disturbed regions) or accurately represent local mechanisms in cracked reinforced concrete (for example, bond-slip effects, and stress condition at the crack). Compared to beam elements, membrane elements can capture detailed mechanisms and compute the response of the structure with better accuracy. However, modeling the entire structure with membrane elements is typically not practical due to computational time and memory storage limitations. With a mixed-type modeling approach, a combination of beam elements and membrane elements can be used to model the entire structure while taking into account local effects in critical members and members with complex or continuum-type of behavior. This requires having a good understanding of the structural behavior and recognizing the location of the critical regions prior to the analysis.

For coupling a beam element with membrane elements, special consideration must be given in modeling the interface section. Specifically, the rotation at the interface node of the beam element must be transferred to the equivalent displacements of membrane elements, which usually only support translational degrees-of-freedom (DOFs). The procedure must satisfy compatibility and equilibrium requirements at the interface section. In addition, because the interface section is usually located close to a critical member of the structure and the distance, which is influenced by coupling the two elements is not known prior to the analysis, realistic stress distributions must be computed at the interface section.

The existing beam-membrane coupling methods can be categorized into three main types: rigid links, multi-point constraints (MPCs), and transition elements. Rigid links are the simplest type of coupling method in which extremely high stiffness members connect beam and membrane elements.^{1,2} Although the rigid links method satisfies compatibility and equilibrium requirements, it does not provide a realistic stress distribution at the interface section. In addition, a set of transverse rigid members at the connection acts as a strong stirrup that does not allow transverse expansion at the interface, adding additional stiffness to the structure, which may affect the response of the system.

With the MPC methods, constraint equations define the relationship between the displacements at the interface DOFs of the beam and membrane elements. One popular type of MPC method is the energy-based approach proposed by McCune et al.³ In this method, the constraint equations were derived based on equating the work done by the stresses in each element type at the interface and the assumed stress distributions along the cross section. Ho et al.⁴ proposed constraint formulations based on defining equivalent forces and moment for the beam element at the connection section. Although the method resulted in a uniform and unperturbed stress distribution between the two types of elements, it assumed rigid displacements, which did not allow transverse expansion at the interface section. Wang et al.⁵ used the virtual work concept and developed an iterative procedure to formulate constraint equations by applying unit forces and moment on the beam submodel. While the method eliminated the stress distribution assumptions made in previous

ACI Structural Journal, V. 115, No. 3, May 2018.

MS No. S-2017-199, doi: 10.14359/51701130, was received May 31, 2017, and reviewed under Institute publication policies. Copyright © 2018, American Concrete Institute. All rights reserved, including the making of copies unless permission is obtained from the copyright proprietors. Pertinent discussion including author's closure, if any, will be published ten months from this journal's date if the discussion is received within four months of the paper's print publication.

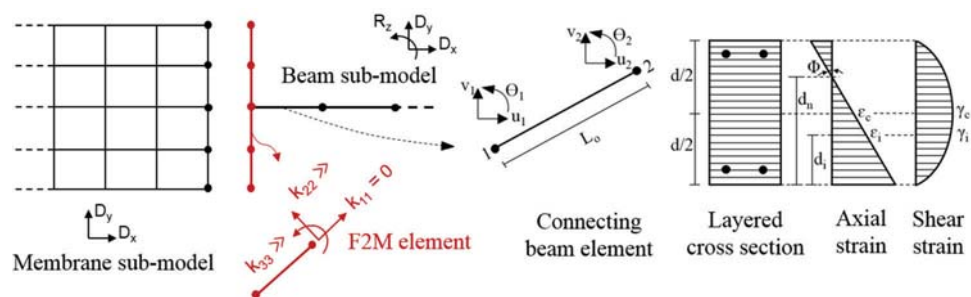


Fig. 1—Overview of F2M element and strain distributions through cross section at interface section.

MPC methods, the expensive computations required to update the constraint equations prohibited its practical application to nonlinear analysis.

Another type of coupling method is based on the use of transition elements. Most of the research in this area has been focused on shell-solid connections. For the beam-membrane coupling problem, Bathe⁶ proposed a transition element based on isoparametric finite element formulation of a one-dimensional (1-D) beam element. Kim and Hong⁷ introduced a two-dimensional (2-D) transition element for analysis of coupled frame-shear wall structures. The stiffness matrix of the transition element was formulated based on constraint equations that assumed linear and constant displacement distributions in the axial and vertical directions, respectively. Garusi and Tralli⁸ proposed a hybrid set of stress-assumed transition elements for beam-solid and beam-shell connections. Instead of formulating the stiffness matrix using relationships between displacements of DOFs, the method derived stiffness properties by assuming a stress field based on the Saint-Venant theory. However, these transition elements were prone to “spurious kinematic modes” that had to be suppressed through the introduction of a penalty strain energy term.

While the afore-mentioned beam-membrane coupling methods can satisfy the compatibility and equilibrium requirements at the interface section, they have limitations when applied to nonlinear analysis of reinforced concrete structures. Some of the methods impose a constant transverse displacement distribution that does not allow for transverse expansion and accurate calculation of Poisson’s effects.^{1,2,4,6,7} Some of the methods do not consider stress distribution at the interface^{1,2,6,7} and the ones that do, analyze the effects of axial stresses and shear stresses separately.³⁻⁵ However, in reinforced concrete structures, the axial and shear stresses are closely interrelated (for example, stress condition at the crack). Also, almost all the previous studies have focused on linear elastic analysis, but the behavior of reinforced concrete structures is highly nonlinear due to the low cracking strength and nonlinear compression response of the concrete, and yielding of the reinforcement.

In this study, a new beam-membrane (that is, frame-membrane) interface element, named the F2M element, is developed particularly for the analysis of reinforced concrete structures with an attempt to address the aforementioned limitations. An iterative procedure, formulated based on the Disturbed Stress Field Model (DSFM),⁹ is used to calculate linear and nonlinear stress distributions at the interface

section. The procedure allows for transverse expansion and accounts for Poisson’s effects at the interface section. The performance of the F2M element is examined by mixed-type modeling of a series of beam specimens and comparing the results against experimental tests, stand-alone models, and two other commonly used coupling methods. In addition, to demonstrate the application of the F2M element, a reinforced concrete frame structure with critical joints is modeled and analyzed in a mixed-type manner.

RESEARCH SIGNIFICANCE

Integration of advanced membrane elements with computationally fast beam elements is an effective solution technique for multi-scale analysis of large, complex structures. The existing beam-membrane coupling methods are mostly limited to linear elastic problems and have several major deficiencies when applied to reinforced concrete members (for example, considering the transverse expansion or the shear strength reduction due to the concrete cracking). This study presents a new type of beam-membrane interface element that eliminates limitations of the existing coupling methods and improves modeling of the connecting section. In multi-scale analysis, accurate modeling of the connecting section, which is typically located close to a deficient member, can influence both the local and global behavior of the structure.

PROPOSED INTERFACE ELEMENT

Overview

The F2M interface element is a two-noded semi-deformable element that has to be used as a group of elements oriented perpendicular to the beam element and along the membrane elements at the connecting section. The algorithm of the proposed element includes three main parts: 1) stiffness of the element; 2) axial and shear stress distributions; and 3) nonlinear material models. A comprehensive description of each part is provided in the following subsections.

As shown in Fig. 1, the stiffness matrix of the F2M element is set such that it has high stiffness values in the transverse and rotational directions (K_{22} and K_{33} , respectively) and near-zero stiffness in the axial direction (K_{11}). This enables the analysis to transfer the rotation from the beam elements to the equivalent translational displacements in the membrane elements based on the assumption that “plane sections remain plane.” In addition, having near-zero stiffness in the axial direction avoids the addition of extra stiffness to the system and allows lateral expansion at the connecting section. In a typical coupling method, the shear

forces are transferred between the two elements using either the rigid links or a predefined stress distribution at the interface section. With the F2M element, because the axial stiffness is set to a near-zero value, an iterative procedure is used to compute shear and axial stress distributions at the interface section. The procedure accounts for the material nonlinearity effects based on the DSFM model.

Stress distributions

An iterative procedure is used to transfer shear between the two submodels. The procedure is adopted from frame analysis software developed by Guner and Vecchio.¹⁰ In the first iteration of the analysis, the solution of the structural system is calculated assuming high stiffness in the axial direction for the F2M elements (that is, F2M elements initially act similarly to those in the rigid links method). In the subsequent iterations, the axial stiffness of the F2M elements is set to a near-zero value. Using a layered analysis approach that assumes plane sections remain plane, the longitudinal strains at each layer of the cross section can be calculated from the change in the length and curvature of the connecting beam element (refer to Fig. 1)

$$\epsilon_{c,p} = \frac{L_p - L_o}{L_o} \quad (1)$$

$$\phi_p = \frac{\theta_{1,p} + \theta_{2,p}}{L_o} \quad (2)$$

$$\epsilon_{i,p} = \epsilon_{c,p} + \phi_p \left(\frac{d}{2} - d_i \right) \quad (3)$$

where θ_1 and θ_2 are the rotations at the two ends of the connecting beam element; d and d_i are the heights of the cross section and i -th layer; L_o is the initial length of the element; L_p and ϕ_p are the length and curvature of the element at iteration p ; and ϵ_c and ϵ_i are the axial strains at middepth and i -th layer of the cross section, respectively. Using the computed shear force from the structural system solution, the shear strain at the middepth of the element ($\gamma_{c,p}$) can be estimated for elastic members as

$$\gamma_{c,p} = SF \frac{V}{G_c \cdot A_t} \quad (4)$$

where V is the shear force; G_c is the elastic shear modulus as given by Eq. (5); A_t is the transformed cross-sectional area; and SF is the shear area factor for elastic members, which is taken as 1.20 and 1.11 for rectangular sections and circular sections, respectively, as suggested by Gere and Timoshenko¹¹

$$G_c = \frac{E_c}{2(1+\nu)} \quad (5)$$

In Eq. (5), E_c and ν are the modulus of elasticity and the Poisson's ratio of the concrete, respectively. Knowing the

shear strain at the middepth of the cross section and assuming a parabolic shear strain distribution, the shear strain of each layer at iteration p of the analysis can be determined as

$$\gamma_{i,p} = \frac{4\gamma_{c,p}}{d^2} (dd_i - d_i^2) \quad (6)$$

The stress-strain constitutive relationship at the interface section can be written as:

$$\begin{Bmatrix} \sigma_x \\ \sigma_y \\ \tau_{xy} \end{Bmatrix} = \begin{bmatrix} D_{11} & D_{12} & D_{13} \\ D_{21} & D_{22} & D_{23} \\ D_{31} & D_{32} & D_{33} \end{bmatrix} \times \begin{Bmatrix} \epsilon_x \\ \epsilon_y \\ \gamma_{xy} \end{Bmatrix} - \begin{Bmatrix} \sigma_x^o \\ \sigma_y^o \\ \tau_{xy}^o \end{Bmatrix} \quad (7)$$

where $\{\sigma\}$ and $\{\epsilon\}$ are the total stress and strain vectors; $[D]$ is the composite material stiffness matrix; and $\{\sigma^o\}$ is the pseudo-stress vector corresponding to the strain offsets as defined in the DSFM model.

The total strains in concrete can be expressed as a composition of: 1) net strains $\{\epsilon_c\}$, which are used for calculations of stresses and stiffness moduli in the concrete; 2) elastic offset strains $\{\epsilon_c^o\}$ due to lateral expansion, thermal, shrinkage, and prestrain effects; 3) plastic offset strains $\{\epsilon_c^p\}$ due to permanent deformation resulting from cyclic loading; and 4) crack slip offset strains $\{\epsilon_c^s\}$ due to shear slip on the crack. The total concrete strains can be represented as

$$\{\epsilon\} = \{\epsilon_c\} + \{\epsilon_c^o\} + \{\epsilon_c^p\} + \{\epsilon_c^s\} \quad (8)$$

Assuming perfect bond between the reinforcement and the concrete, the total strains developed in the i -th reinforcement component are equal to the total strains of the concrete at the same location. Therefore, in a similar manner, the total strains in the reinforcement can be expressed as a summation of: 1) net strains $\{\epsilon_s\}$, which are used for calculations of the stress and stiffness modulus in the reinforcement; 2) elastic offset strains $\{\epsilon_s^o\}$ due to thermal and prestrain effects; and 3) plastic offset strains $\{\epsilon_s^p\}$ due to steel yielding and damage resulting from cyclic loading. The total reinforcement strains can be written as

$$\{\epsilon\}_i = \{\epsilon_s\}_i + \{\epsilon_s^o\}_i + \{\epsilon_s^p\}_i \quad (9)$$

Because of the perfect bond assumption, the proposed interface element should be located an adequate distance from sections with critical bond-slip behavior (for example, interface of beam and column in joint panels). The distance, which is influenced by coupling the two types of elements, can be determined using a sensitivity analysis.

The pseudo-stress vector $\{\sigma^o\}$ is computed from the summation of the pseudo-stress vector arising from strain offsets of the concrete, $\{\sigma_c^o\}$, and the pseudo-stress vectors resulting from strain offsets of all the reinforcement components, $\{\sigma_s^o\}$

$$\{\sigma^o\} = \{\sigma_c^o\} + \sum_{i=1}^n \{\sigma_s^o\}_i \quad (10)$$

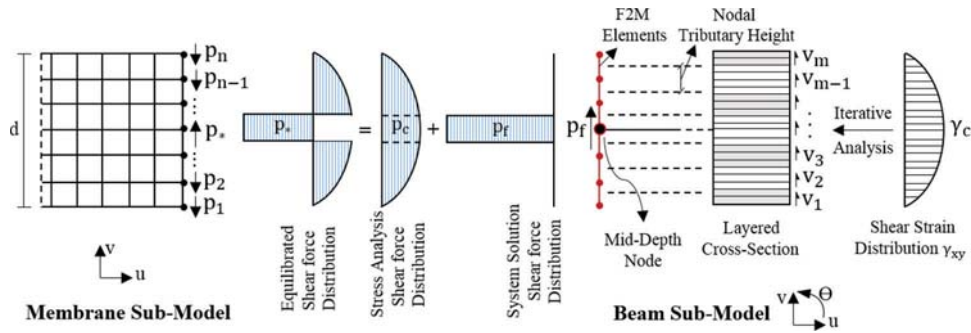


Fig. 2—Transferring shear forces between beam and membrane elements.

$$\{\sigma_c^o\} = [D_c] \times (\{\epsilon_c^o\} + \{\epsilon_c^p\} + \{\epsilon_c^s\}) \quad (11)$$

$$\{\sigma_s^o\}_i = [D_s]_i \times (\{\epsilon_s^o\}_i + \{\epsilon_s^p\}_i) \quad (12)$$

where $[D_c]$ and $[D_s]_i$ are the material stiffness matrices for the concrete and the i -th reinforcement component, respectively.

Assuming zero clamping stress at the interface section ($\sigma_y = 0$), an iterative procedure can be used to calculate the axial stress (σ_x) and shear stress (τ_{xy}) at each layer of the cross section without decoupling the effects of stresses. First, the axial strain (ϵ_x) and shear strain (γ_{xy}) are determined from Eq. (3) and (6), respectively. Assuming $[D_c]$ and $[D_s]_i$ are known matrixes (developments presented in the next section), $\{\sigma^o\}$ can be computed from Eq. (10) to (12) using the strain offsets. Thus, the constitutive relationship, Eq. (7), can be simplified to three equations and three unknowns in which the unknowns are the axial stress (σ_x), shear stress (σ_{xy}), and transverse strain (ϵ_y). Solving Eq. (7) provides the axial and shear stress distributions at the beam side of the interface section. Using the computed shear stress distribution and the tributary area concept, the equivalent axial forces at the F2M element nodes are computed. To transfer shear between the two submodels, the computed equivalent forces are applied in the opposite direction on the corresponding nodes of the connecting membrane elements.

To satisfy equilibrium at the interface section, the computed force of the membrane node located at the cross-sectional middepth must be modified to account for the total shear force carried by the corresponding node in the frame submodel resulting from the system-level analysis. Without this force modification, the sectional shear force will be counted twice—once from the shear force carried by the connecting node of the frame submodel, and once from the external forces applied on the connecting nodes of the membrane submodel. As presented in Fig. 2 and Eq. (13), this modified force (P_*) is equal to the difference between the total shear force (P_f) and the equivalent force of the membrane node at the cross-sectional middepth (P_c) and must be applied in the opposite direction of the equivalent force

$$P_* = P_f - P_c \quad (13)$$

Without this force modification, the shear force at the interface section will be twice the correct value.

Material matrix formulation

To compute the composite material stiffness matrix $[D]$ in the aforementioned iterative procedure, the behavior of cracked reinforced concrete is represented according to the DSFM model. This model is formulated based on the smeared rotating crack approach, where the cracks are considered as an average deformation spread out over the area of the finite elements. In the iterative procedure, first, an arbitrary value is assumed for the transverse strain (ϵ_y). Knowing all three strain components in the X- and Y- coordinate system, the concrete principal strains (ϵ_{c1} and ϵ_{c2}) can be calculated

$$\epsilon_{c1}, \epsilon_{c2} = \frac{(\epsilon_{cx} + \epsilon_{cy})}{2} \pm \frac{1}{2} \sqrt{(\epsilon_{cx} - \epsilon_{cy})^2 + \gamma_{cxy}^2} \quad (14)$$

Using available stress-strain relationships for concrete and steel, the concrete stresses in the principal directions (f_{c1} and f_{c2}) and the steel stress in the direction of each reinforcing bar component (f_{si}) can be computed. In this study, the constitutive formulations presented in the DSFM model are applied.

Based on the computed stresses and strains in the principal directions, the composite material stiffness matrix $[D]$ can be constructed by superposition of the material stiffness matrixes of the concrete and all the reinforcement components

$$[D] = [D_c] + \sum_{i=1}^n [D_s]_i \quad (15)$$

The concrete material stiffness matrix is calculated using effective secant moduli (\bar{E}_{c1} , \bar{E}_{c2} , \bar{G}_c) defined with respect to the principal directions

$$[D_c]' = \begin{bmatrix} \bar{E}_{c1} & 0 & 0 \\ 0 & \bar{E}_{c2} & 0 \\ 0 & 0 & \bar{G}_c \end{bmatrix} \quad (16)$$

$$\bar{E}_{c1} = \frac{f_{c1}}{\epsilon_{c1}}; \bar{E}_{c2} = \frac{f_{c2}}{\epsilon_{c2}}; \bar{G}_c = \frac{\bar{E}_{c1} \times \bar{E}_{c2}}{\bar{E}_{c1} + \bar{E}_{c2}} \quad (17)$$

The $[D_c]'$ matrix can be transformed back to the X- and Y-axes

$$[D_c] = [T_c]^T [D_c]' [T_c] \quad (18)$$

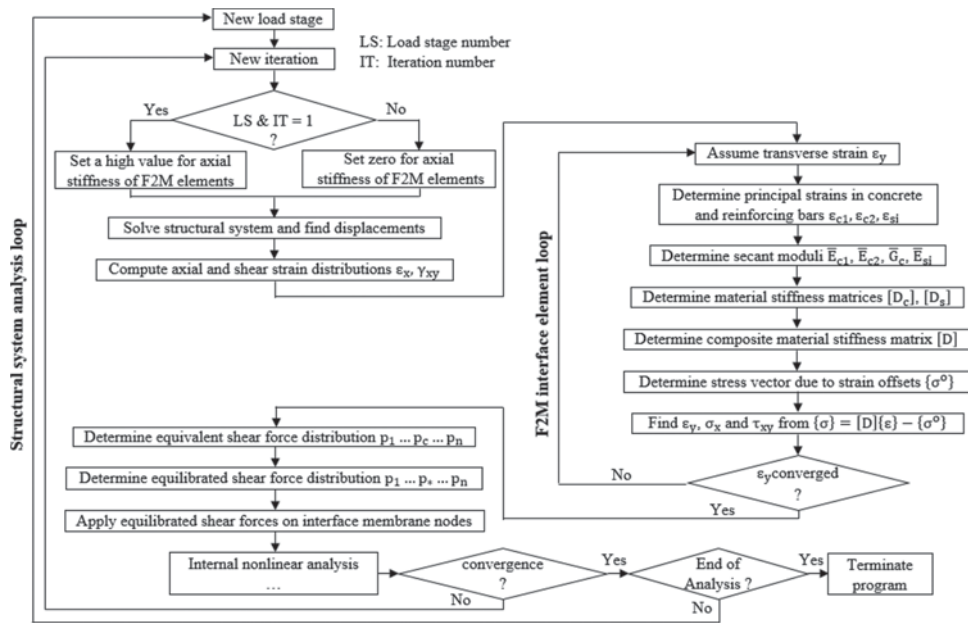


Fig. 3—Algorithm of proposed beam-membrane interface element.

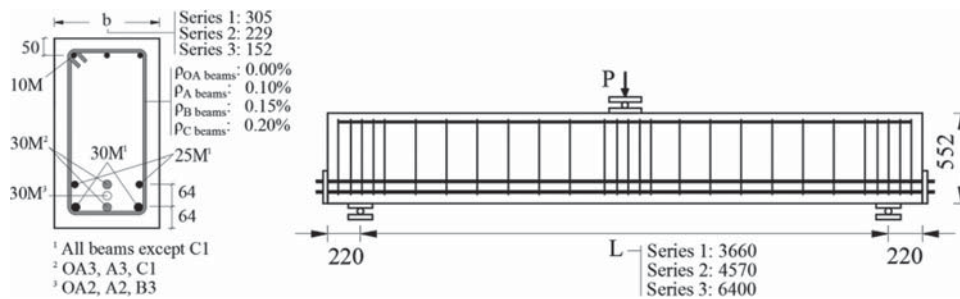


Fig. 4—Details of Vecchio-Shim beams. (Note: Dimensions in mm; 1 mm = 0.0394 in.)

where $[T_c]$ is the transformation matrix described by Cook et al.¹²

The contribution from the i -th reinforcement component to the material stiffness matrix is defined as

$$[D_s]_i = \begin{bmatrix} \rho_{si} \bar{E}_{si} & 0 & 0 \\ 0 & 0 & 0 \\ 0 & 0 & 0 \end{bmatrix} \quad (19)$$

$$\bar{E}_{si} = \frac{f_{si}}{\epsilon_{si}} \quad (20)$$

where ρ_{si} is the reinforcement ratio; ϵ_{si} is the reinforcement strain; and E_{si} is the effective steel modulus for i -th reinforcement component. Using a similar transformation matrix applied to the concrete material stiffness, $[D_s]_i$ can be transferred from the longitudinal axis of the reinforcing bar to the X- and Y-reference axes

$$[D_s]_i = [T_s]_i^T [D_s]_i' [T_s]_i \quad (21)$$

Knowing the composite material stiffness matrix $[D]$, the stress-strain constitutive equation, Eq. (7), can be solved to determine new values of the transverse strain (ϵ_y). The procedure is repeated until the transverse strain (ϵ_y) values

converge within a predefined error limit. After the convergence has been achieved, the computed shear stress (τ_{xy}) values can be used to determine equivalent shear forces. Figure 3 indicates the main steps of the proposed beam-membrane coupling method.

VERIFICATION STUDY

The verification study was performed on a series of 12 simply supported beams tested by Vecchio and Shim¹³ under a monotonic loading condition. The beams were categorized into three series of tests (Series 1, 2, and 3) according to their clear span length (3.66, 4.57, and 6.40 m, [4, 5, and 7 yd] respectively). Each series of tests comprised four beam specimens with a different cross-sectional width and reinforcement configuration (Beams OA, A, B, and C). The beams had light amounts of transverse reinforcement, ranging from 0.0% to 0.2%. Three different failure modes were observed during the experiment: diagonal-tension, shear-compression, and flexural-compression. The cross section and elevation details of the beams are presented in Fig. 4.

Finite element models

Stand-alone models—Two types of stand-alone models were created for each beam: a frame model (analyzed with VecTor5 program¹⁴) and a membrane model (analyzed with VecTor2 program¹⁵). Taking advantage of the symmetry of

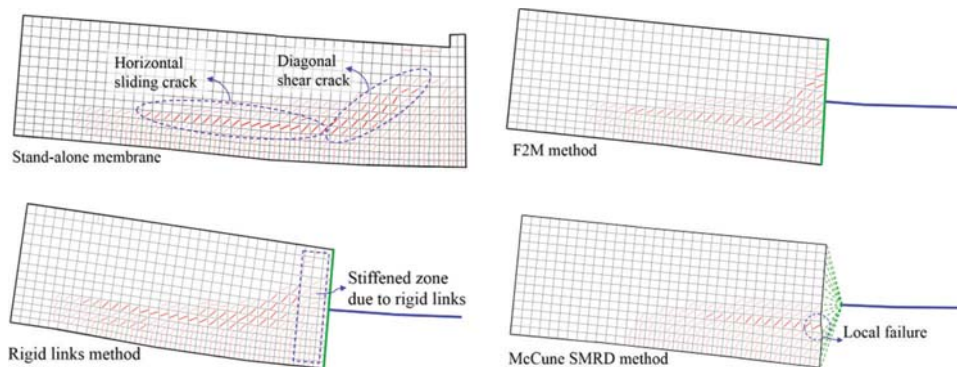


Fig. 5—Comparison of crack patterns of OA1 beam based on different mixed-type methods.

the beams and test setup, only half of the beam span was modeled. In the stand-alone frame analysis, 6-DOF layered frame elements with element lengths ranging from 200 to 300 mm (7.87 to 11.81 in.) were used to model the beams. Each frame element was divided into 50 concrete layers, providing sufficient accuracy for the sectional analysis. The loading was applied as an imposed displacement with increments of 0.25 mm (0.01 in.) at the midspan of the beam. To model the support conditions, a roller support was defined at the left end of the beam by restraining the vertical DOF. In addition, to satisfy the condition of symmetry, both the horizontal and rotational DOFs were restrained at the midspan nodes of the beam.

The stand-alone membrane model was created using 8-DOF reinforced concrete rectangular elements with an approximate mesh size of 45 x 37 mm (1.77 x 1.46 in.) in the X- and Y-directions, respectively. Longitudinal reinforcing bars were modeled as discrete using 4-DOF truss bar elements; the transverse reinforcement was modeled as smeared. The loading plate was modeled using structural steel rectangular elements. Between the steel and concrete elements, a layer of unidirectional bearing elements was used to allow strain in the horizontal direction, providing a more realistic representation of the force distribution and crack pattern under the load.

Mixed-type models—For the beams without shear reinforcement (OA1, OA2, and OA3), the behavior was dominated by a diagonal-tension crack that continued as a sliding crack in the horizontal direction along the longitudinal reinforcement extending to the support (refer to Fig. 5). To accurately capture the failure mechanism, the membrane submodel was created on the support side of the beam and the frame submodel was created on the midspan side of the structure. Two types of mixed-type models were used: Mixed-Type 1 (0.65L membrane submodel and 0.35L frame submodel), and Mixed-Type 2 (0.90L membrane submodel and 0.10L frame submodel), where L is the half-span length of the beam.

With the other types of the beams (A, B, and C), which contained transverse reinforcement, the failure was initiated by crushing of the concrete in the compression zone under the loading plate, which was followed by either a diagonal shear crack (Series 1 and 2) or flexural cracks at the midspan (Series 3). For these beams, because the location of the critical zones varied depending on the type of failure, two types of mixed-type models with opposite substructuring configurations

were created (Mixed-Type 1 and Mixed-Type 2). In the Mixed-Type 1 configuration, the membrane submodel was located close to the support end of the beam, while in the Mixed-Type 2 configuration, the membrane submodel was located near the loading plate. In both mixed-type models, 65% of the structure was modeled using membrane elements and 35% of the structure was modeled with frame elements.

The two submodels were connected using the proposed interface elements. A newly developed simulation framework, named Cyrus,¹⁶ was used to combine the two programs and coordinate the analysis. Figure 6 shows the stand-alone and mixed-type finite element models.

It should be noted that the selected percentages for the length of the submodels (10% and 90% or 35% and 65%) are arbitrary numbers. Different length percentages and substructure configurations are used to demonstrate their influence on the structural behavior. In general, to have optimal results, the membrane submodel must include the critical regions and must be extended adequately to reduce possible stress fluctuations.

Comparison of results

Comparison against stand-alone analyses—The load-deflection responses of the mixed-type analyses are compared against the stand-alone analysis results and experimentally observed behaviors in Fig. 7.

Based on the stand-alone analysis results, both VecTor2 (membrane model) and VecTor5 (frame model) were capable of computing the peak load capacity of the beams with a high level of accuracy. It is worth noting that most other frame-type analysis tools, unlike the VecTor5 program, do not consider shear-related mechanisms, which can result in significant overestimation of the load capacity and ductility. Although VecTor5 was capable of considering shear behavior relatively well, because of the limitations associated with its frame-type analysis nature, it underestimated the ductility and was unable to accurately capture the post-peak response. These facets were computed with much better accuracy by VecTor2, which uses more advanced types of elements.

For all types of mixed-type analyses, except the Mixed-Type 2 configuration of the A beams, the load-deflection responses fell between the stand-alone analysis results of the membrane model and the frame model or were sufficiently close to them, resulting in a high level of accuracy in capturing the behavior of the beams. Also for all mixed-

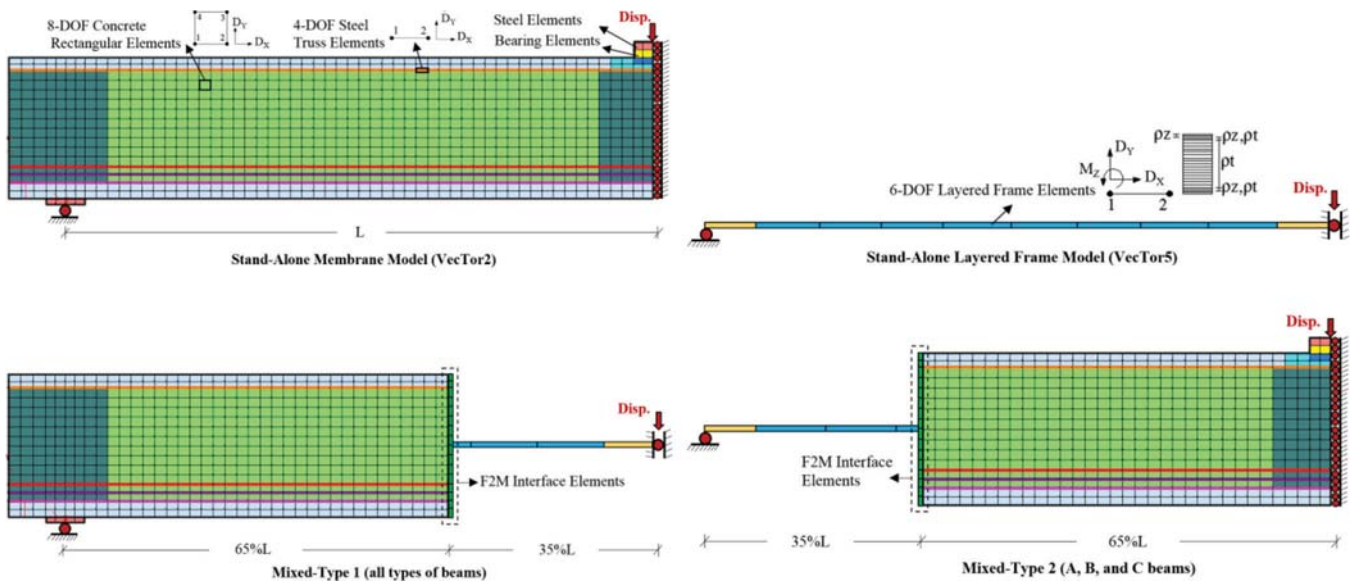


Fig. 6—FE model for stand-alone and mixed-type analyses of Vecchio-Shim beams.

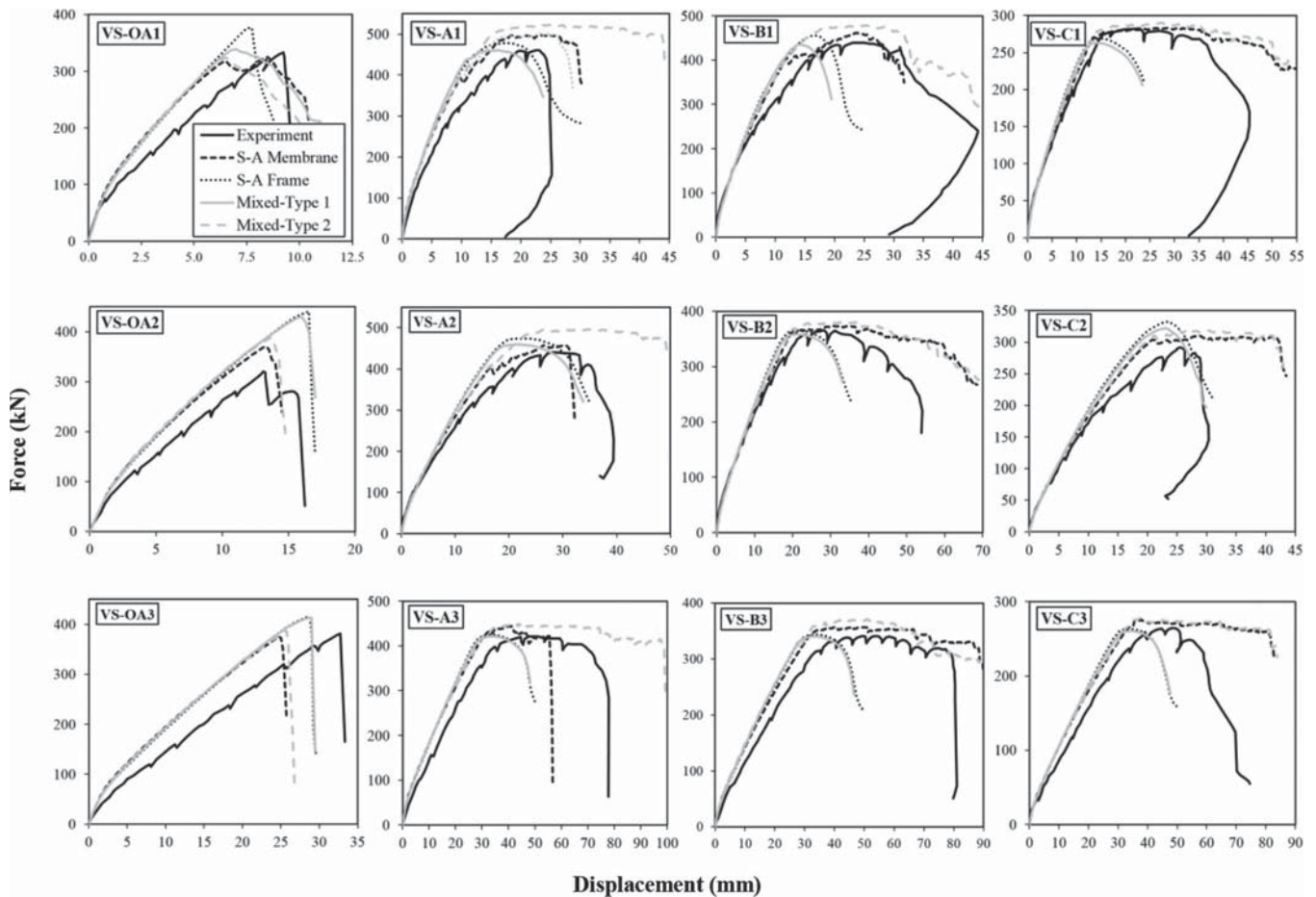


Fig. 7—Comparison of midspan load-deflection responses for Vecchio-Shim beams. (Note: 1 mm = 0.0394 in.; 1 kN = 0.225 kip.)

type analysis cases, the location of the diagonal shear crack was consistent with the location of the critical section for checking the shear capacity of a member as defined in the CSA A23.3 standard¹⁷ (that is, effective shear depth d_v from the support or loading plate). A more detailed description of the analysis results for each type of cross section is provided in the following discussion.

For the OA beams containing no shear reinforcement, the F2M interface element was able to compute the diagonal shear crack at the connection section and the sliding crack in the horizontal direction along the longitudinal reinforcement (refer to Fig. 5). In the Mixed-Type 1 configuration, the shear failure occurred in the frame submodel, resulting in a response that was closer to the stand-alone frame analysis. In

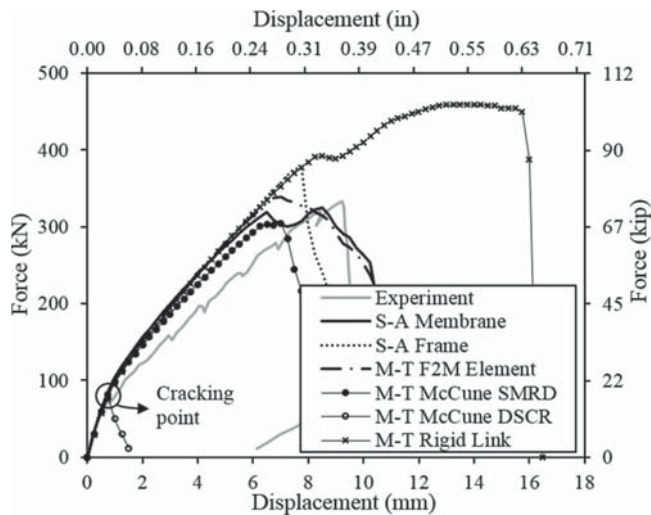


Fig. 8—Load-deflection responses of OA1 beam based on different mixed-type methods.

the Mixed-Type 2 configuration, in which a greater portion of the structure was modeled with membrane elements, the shear failure occurred in the membrane submodel and, therefore, the response leaned toward the stand-alone membrane analysis.

The A beams, having the lowest amount of shear reinforcement among the beams containing stirrups ($\rho_t = 0.1\%$), exhibited the most challenging behavior to capture using the mixed-type analysis. In these beams, all the three types of mechanisms contributed to the final failure. In the Mixed-Type 1 configuration, the failure was governed by crushing of the top layers of frame elements in the compression zone, leading to a response that was closer to the stand-alone frame analysis. In the Mixed-Type 2 configuration, having the frame submodel on the support side of the beams compromised the ability of the mixed-type analysis to fully capture the horizontal sliding crack, resulting in overestimations of the peak load and ductility.

With the B and C beams, having higher amounts of shear reinforcement ($\rho_t = 0.15\%$ and 0.2% , respectively) compared to the OA and A beams, the influence of the horizontal sliding crack on the response of the structure was insignificant. Consequently, the analysis results computed by both the Mixed-Type 1 and Mixed-Type 2 configurations had excellent agreement in terms of the peak load and ductility with the stand-alone analysis responses and correlated reasonably well with the experimentally observed behavior. Depending on whether the critical region of the beam was located in the membrane submodel or the frame submodel, the mixed-type analysis response followed a similar path as the stand-alone membrane or frame analysis response.

A more detailed comparison of the results in terms of the peak load and corresponding displacement values is provided by Sadeghian.¹⁸

Comparison against other mixed-type methods—To further assess the performance of the F2M interface element, the analysis results were compared against two other existing coupling methods that have been widely used in previous studies: the Rigid Links method^{1,2} and the McCune et al. method.³ The investigation was conducted on the Mixed-Type 1 model of Beam OA1, which exhibited a dominant

shear behavior in both the stand-alone analysis and in the experiment.

The midspan load-deflection responses and crack patterns computed by different types of mixed-type methods are presented in Fig. 8 and Fig. 5, respectively. In Fig. 8, the accuracy of different mixed-type models should be evaluated based on the response of the stand-alone membrane model rather than the experiment; the stand-alone membrane model is the most accurate analysis that can be obtained using the VecTor2 and VecTor5 programs. It can be seen that the Rigid Links method greatly overestimated the peak load and ductility of the beam due to the use of high stiffness elements at the connection section between the two submodels. A set of high stiffness elements located along the height of the section performed as a strong stirrup that suppressed the formation of a diagonal shear crack at the interface section.

The McCune et al. method³ computed the linear response of the structure well; however, as expected, after cracking of the concrete, it failed to capture the behavior of the beam, resulting in a significant stress concentration at the longitudinal reinforcement layer and consequently a premature local failure. To investigate the McCune et al. method³ in more detail, another mixed-type model was created in which the longitudinal reinforcement was modeled as smeared in a tributary area of approximately 7.5 times the bar diameter, as recommended by CEB-FIP.¹⁹ Although this prevented the local failure at the longitudinal reinforcement layer, the analysis response underestimated the stiffness and peak load compared to the stand-alone analysis results. In addition, the analysis was not able to capture the diagonal shear crack and computed a horizontal crack located at approximately the middepth of the elements containing smeared longitudinal reinforcement. It is worth reiterating that the McCune et al. method³ was developed for linear elastic problems and was not intended to be applicable to nonlinear analysis of reinforced concrete structures.

Unlike the other two mixed-type methods, the F2M interface element computed a load-deflection response that was between the stand-alone detailed FE analysis and the stand-alone frame analysis results. With respect to the crack pattern, the F2M element was able to capture the diagonal shear crack at the connection section and also the horizontal sliding crack along the longitudinal reinforcement layer.

The computed stress distributions at the interface section of the membrane submodel for pre- and post-cracking conditions are presented in Fig. 9 and 10, respectively. For the proposed F2M element, prior to cracking, the computed axial and shear stresses are almost identical to the stand-alone membrane model. After cracking of the concrete, the F2M element was able to accurately capture the stress reduction in the cracked elements located at the bottom of the cross section and the increase in stresses of the uncracked elements at the top of the cross section. Compared to the stand-alone membrane model, the axial stresses correlated very well and the shear stresses were reasonably accurate. For the vertical stresses, the proposed procedure assumes no clamping stress at the interface section. However, the external forces applied through the section to transfer the

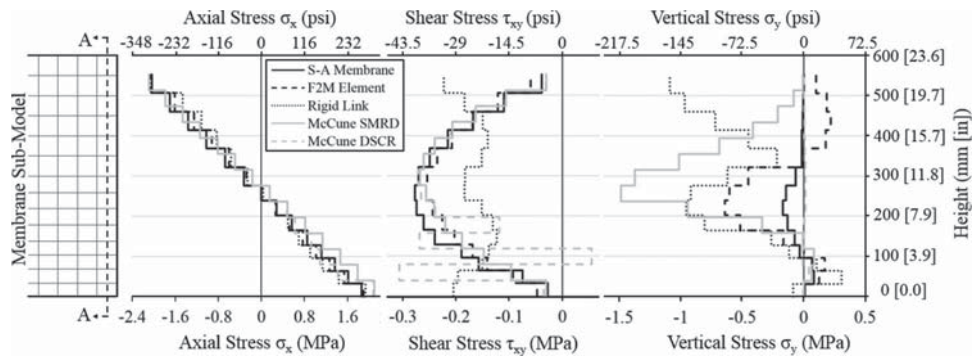


Fig. 9—Stress distributions through section prior to cracking (applied displacement = 0.5 mm [0.02 in.]).

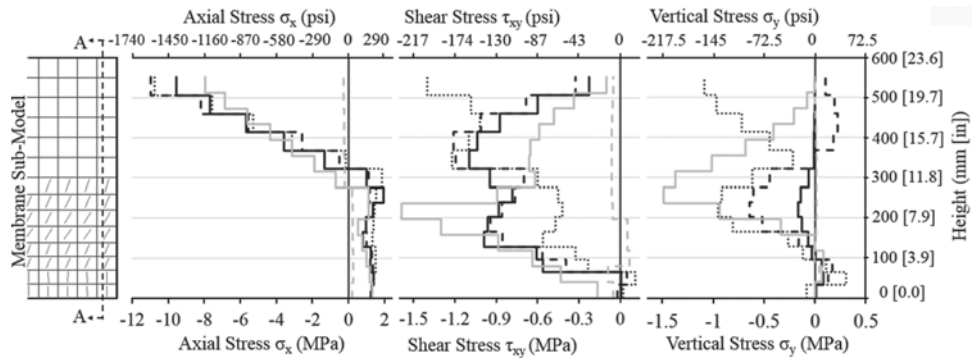


Fig. 10—Stress distributions through section after cracking (applied displacement = 4.0 mm [0.16 in.]).

shear force between the two submodels can cause some fluctuations in the vertical stress distribution. It is worth noting that the amount of overestimation of the vertical stresses computed by the F2M method is much less than that of the other two coupling methods.

The other two coupling methods showed major limitations in determining the interface stresses. Although the Rigid Links method accurately captured the axial stresses in both pre- and post-cracking conditions, the computed shear and vertical stresses appeared to have random distributions. Prior to cracking, the McCune et al. method³ was unable to capture the shear stresses of concrete membrane elements that were connected to truss elements representing reinforcing bars (that is, discrete modeling). Alternatively, the longitudinal reinforcing bars were modeled as a component of membrane elements (that is, smeared modeling). While the smeared modeling approach produced a correct shear stress distribution, it limits considering some of the mechanisms such as bond-slip effects, which can be critical in other types of structures. After cracking of the concrete, both the smeared and discrete models of the McCune et al. method³ were unable to accurately capture the shear stress distribution.

APPLICATION EXAMPLE

The application of the proposed interface element and advantages of using the mixed-type analysis method are demonstrated through modeling a reinforced concrete frame structure previously tested by Calvi et al.²⁰ The frame was designed for gravity loads only based on typical Italian construction practice common in 1970s (that is, smooth reinforcing bars, no stirrups in the joints, and the longitudinal bars in the exterior joints anchored with short, 180-degree

end-hooks). The lateral loads were applied in a hybrid force-displacement control manner; the displacement at the top floor was increased in a reversed cyclic regime while maintaining a linear force distribution along the height of the structure. In addition, a gravity load of 73 kN (16.41 kip) was applied on the first and second floors, and 54.2 kN (12.18 kip) was imposed on the third floor. Dimensions of the frame and imposed loads are shown in Fig. 11. According to the test results, the poor detailing of the reinforcement led to a brittle failure mode with most of the damage concentrated in the exterior beam-column joint regions of the first floor.

Stand-alone model

A frame model of the entire structure was analyzed using VecTor5. The modeling procedure was similar to that described for the beam specimens in the Verification Study section. A total of 338 layered beam elements each divided into 30 layers were used. The joint regions were represented with stiffened elements to avoid artificial damage. The gravity loads were modeled as nodal and element forces representing the externally applied loads and self-weight of the structure, respectively. Because the hybrid force-displacement type of loading is not available in VecTor5, instead of applying the lateral loads in a reversed cyclic manner, a pushover analysis was performed. The lateral loads were modeled with nodal forces and monotonically increased up to the failure point in increments of 0.5 kN (0.112 kip).

The load-deflection response of the push-over analysis is compared to the experimentally observed behavior in Fig. 12(a). The stand-alone frame analysis response agreed reasonably well with the experimental results up to the point where the joints began to crack. However, beyond this point,

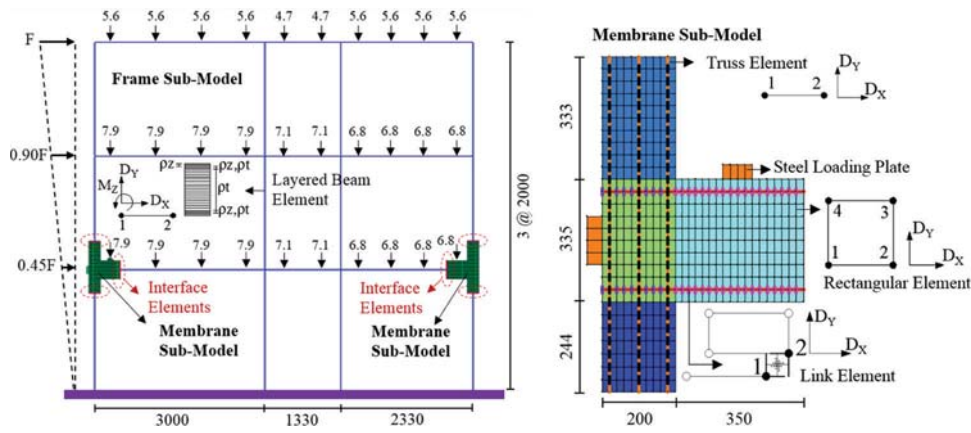


Fig. 11—Mixed-type model of frame. (Note: Dimensions in mm and forces in kN; 1 mm = 0.0394 in.; 1 kN = 0.225 kip.)

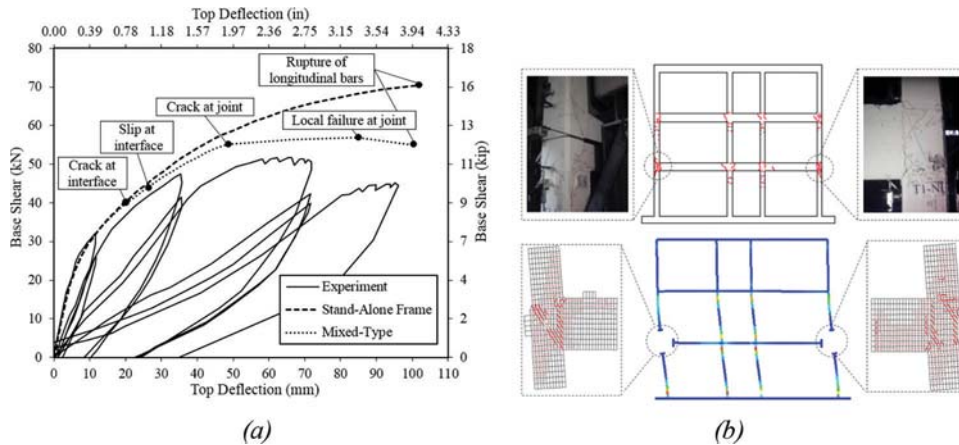


Fig. 12—Experimental and analytical: (a) load-deflection responses; and (b) crack patterns for frame.

due to the limitations of the beam elements, the analysis began to overestimate the strength and stiffness, resulting in much higher failure load than the experiment.

Mixed-type model

A more accurate response of the structure can be obtained using a mixed-type model, where the critical regions (external joints in the first floor) were modeled using membrane elements (VecTor2 program) while the rest of the frame was modeled with layered beam elements (VecTor5 program). The interface between the membrane elements and beam elements was modeled with the F2M element. Cyrus was used to combine the two programs and coordinate the analysis. For the membrane submodel, the modeling procedure was similar to that described for the beam specimens in the Verification Study section. The only difference was defining link elements between rectangular elements and truss elements to capture bond-slip effects. Details of the mixed-type model are shown in Fig. 11.

Based on the load-deflection responses presented in Fig. 12(a), the mixed-type model predicted the peak load and stiffness values much more accurately than the stand-alone analysis. The mixed-type analysis computed a large amount of slip in the longitudinal reinforcement of the beams at the interface section, resulting in a significant reduction in the stiffness of the system. The analysis also showed post-peak decay in strength due to local failure in

the joints. The computed crack pattern agreed well with the experimentally observed behavior (refer to Fig. 12(b)). None of these mechanisms were captured in the stand-alone frame analysis, illustrating the effectiveness of the mixed-type simulation.

It is worth noting that the analysis times of the stand-alone and mixed-type models on a desktop computer with a high-speed processor were approximately 4 and 9 minutes, respectively, which were considered acceptable. Modeling the entire structure with membrane elements results in a much higher analysis time that may not be practical, particularly if a cyclic or a dynamic type of analysis is required.

SUMMARY AND CONCLUSIONS

In this study, a new beam-membrane interface element, the F2M element, which was specifically formulated for mixed-type analysis of reinforced concrete structures, was presented and verified. The procedure satisfies equilibrium and compatibility requirements at the connection section. The main contributions of the proposed interface method, not available in other known mixed-type methods, can be summarized as: 1) computing linear and nonlinear axial and shear stress distributions at the interface section with a high level of accuracy without decoupling the axial, flexural, and shear effects; 2) allowing for transverse expansion and accurate calculation of Poisson's effects at the interface section using offset strains; 3) considering reinforced

concrete as a composite material enabling the use of truss elements in addition to the membrane elements at the interface section. Beside these advantages, the assumptions used in the proposed procedure make it not suitable for coupling elements with high clamping forces or elements located at disturbed regions.

The performance of the F2M element was verified through mixed-type modeling of a series of 12 shear-critical beam specimens which exhibited different types of failure modes. In addition, the application of the F2M element and mixed-type modeling approach was demonstrated by analysis of a frame structure with critical joints. The following conclusions can be drawn from the verification and application examples:

1. Overall, the mixed-type analysis based on the F2M element provided reliable and consistently accurate calculations of initial stiffness, peak load, and ductility of the beams. For all beams considered, using a proper substructuring configuration, the mixed-type analysis results were sufficiently close to the stand-alone analysis results and the experimentally reported values.

2. The F2M element was able to capture the shear failure at the interface section and accurately compute the reduction in stress levels of the cracked concrete elements and, consequently, the increase in the stress values of uncracked elements. This resulted in axial and shear stress distributions which correlated reasonably well with the stand-alone membrane model. Contrary to the F2M element, the Rigid Links method and the McCune et al. method³ had major limitations in capturing both the global and local behavior of cracked reinforced concrete members.

3. Mixed-type modeling of the frame specimen, with proper modeling of the connecting section using the F2M element, enabled detailed analysis of the critical regions (external joints in the first floor) while considering the global response of the structure. Unlike the stand-alone frame model, the mixed-type model was able to capture the damage in the external joints, resulting in a structural response that had a much better correlation with the experimental results.

4. Caution must be taken in using a mixed-type simulation method. Creating a proper mixed-type model requires having a good understanding of the expected behavior of the structure and an anticipation of the location of critical regions prior to the analysis. For a single member structure (for example, beam specimens), this can be difficult; for a multi-member structure (for example, frame specimen), the location of potentially critical member(s) is typically more intuitive.

AUTHOR BIOS

Vahid Sadeghian is a PhD Graduate in the Department of Civil Engineering at the University of Toronto, Toronto, ON, Canada. His research interests include hybrid (experimental-numerical) simulation, multi-platform analysis of reinforced concrete structures, and performance assessment of repaired structures.

Oh-Sung Kwon is an Associate Professor in the Department of Civil Engineering at the University of Toronto. His research interests include hybrid (experiment-analysis) simulation, multi-platform simulation of geotechnical and structural systems, and structural earthquake engineering.

Frank J. Vecchio, FACI, is a Professor in the Department of Civil Engineering at the University of Toronto. He is a member of Joint ACI-ASCE

Committees 441, Reinforced Concrete Columns, and 447, Finite Element Analysis of Reinforced Concrete Structures. His research interests include nonlinear analysis and design of reinforced concrete structures, constitutive modeling, performance assessment and forensic investigation, and repair and rehabilitation of structures.

ACKNOWLEDGMENTS

Financial support provided by IC-IMPACTS (the India-Canada Centre for Innovative Multidisciplinary Partnerships to Accelerate Community Transformation and Sustainability) is gratefully acknowledged.

REFERENCES

1. Abrams, D. P., "Measured Hysteresis Relationships for Small-Scale Beams," Issue 432 of Civil Engineering Studies, University of Illinois, Urbana-Champaign, IL, 1976, 160 pp.
2. Mata, P.; Barbat, A. H.; and Oller, S., "Two-Scale Approach for the Nonlinear Dynamic Analysis of RC Structures with Local Non-Prismatic Parts," *Engineering Structures*, V. 30, No. 12, 2008, pp. 3667-3680. doi: 10.1016/j.engstruct.2008.06.011
3. McCune, R. W.; Armstrong, C. G.; and Robinson, D. J., "Mixed-Dimensional Coupling in Finite Element Models," *International Journal for Numerical Methods in Engineering*, V. 49, No. 6, 2000, pp. 725-750. doi: 10.1002/1097-0207(20001030)49:6<725::AID-NME967>3.0.CO;2-W
4. Ho, R. J.; Meguid, S. A.; Zhu, Z. H.; and Sauve, R. G., "Consistent Element Coupling in Nonlinear Static and Dynamic Analyses Using Explicit Solvers," *International Journal of Mechanics and Materials in Design*, V. 6, No. 4, 2010, pp. 319-330. doi: 10.1007/s10999-010-9139-x
5. Wang, F. Y.; Xu, Y. L.; and Qu, W. L., "Mixed-Dimensional Finite Element Coupling for Structural Multi-Scale Simulation," *Finite Elements in Analysis and Design*, V. 92, No. 1, 2014, pp. 12-25. doi: 10.1016/j.finell.2014.07.009
6. Bathe, K. J., *Finite Element Procedures in Engineering Analysis*, Prentice-Hall, Englewood Cliffs, NJ, 1982, 736 pp.
7. Kim, H.-S., and Hong, S.-M., "Formulation of Transition Elements for the Analysis of Coupled Wall Structures," *Computers & Structures*, V. 57, No. 2, 1995, pp. 333-344. doi: 10.1016/0045-7949(94)00620-1
8. Garusi, E., and Tralli, A., "A Hybrid Stress-Assumed Transition Element for Solid-to-Beam and Plate-to-Beam Connections," *Computers & Structures*, V. 80, No. 2, 2002, pp. 105-115. doi: 10.1016/S0045-7949(01)00172-9
9. Vecchio, F. J., "Disturbed Stress Field Model for Reinforced Concrete: Formulation," *Journal of Structural Engineering*, ASCE, V. 126, No. 9, 2000, pp. 1070-1077. doi: 10.1061/(ASCE)0733-9445(2000)126:9(1070)
10. Guner, S., and Vecchio, F. J., "Pushover Analysis of Shear-Critical Frames: Formulations," *ACI Structural Journal*, V. 107, No. 1, Jan.-Feb. 2010, pp. 63-71.
11. Gere, J. M., and Timoshenko, S. P., *Mechanics of Materials*, Nelson Thornes Ltd., Cheltenham, UK, 1991, 832 pp.
12. Cook, R. D.; Malkus, D. S.; and Plesha, M. E., *Concepts and Applications of Finite Element Analysis*, third edition, John Wiley & Sons Inc., Englewood Cliffs, NJ, 1989, 630 pp.
13. Vecchio, F. J., and Shim, W., "Experimental and Analytical Re-Examination of Classic Concrete Beam Tests," *Journal of Structural Engineering*, ASCE, V. 130, No. 3, 2004, pp. 460-469. doi: 10.1061/(ASCE)0733-9445(2004)130:3(460)
14. Guner, S., and Vecchio, F. J., "User's Manual of VecTor5," Department of Civil Engineering, University of Toronto, Toronto, ON, Canada, 2008, 88 pp.
15. Wong, P. S.; Trommels, H.; and Vecchio, F. J., "VecTor2 and FormWorks User's Manual, 2nd Edition," Department of Civil Engineering, University of Toronto, Toronto, ON, Canada, 2013, 311 pp.
16. Sadeghian, V.; Vecchio, F. J.; and Kwon, O.-S., "An Integrated Framework for Analysis of Mixed-Type Reinforced Concrete Structures," *CompDyn 2015 Conference*, Crete, Greece, 2015.
17. CSA Committee A23.3, "Design of Concrete Structures," Canadian Standard Association, Rexdale, ON, Canada, 2014, 297 pp.
18. Sadeghian, V., "A Framework for Multi-Platform Analytical and Experimental Simulations of Reinforced Concrete Structures," PhD dissertation, Department of Civil Engineering, University of Toronto, ON, Canada, 2017, 301 pp.
19. CEB-FIP, "Model Code for Concrete Structures," Comité Euro International du Béton, Lausanne, Switzerland, 1990, 437 pp.
20. Calvi, G. M.; Magenes, G.; and Pampanin, S., "Experimental Test on a Three Storey RC Frame Designed for Gravity Only," *12th European Conference on Earthquake Engineering*, London, UK, 2002.